

of ubiquitin conjugates from proteasome substrates (32). There exist other Csn5/Rpn11 homologs in eukaryotes (Fig. 1) and, by extension, we propose the "JAMMIN" hypothesis, which posits that eukaryotic JAMM proteins are isopeptidases that deconjugate Nedd8 or other ubiquitin-like proteins.

Drosophila sustained by Csn5 carrying a JAMM domain mutation arrest development as larvae with abnormalities in photoreceptor differentiation, suggesting that at least two functions associated with Csn5—viability and photoreceptor differentiation—require its JAMM-dependent isopeptidase activity. Given that Csn5 has been implicated in c-jun signaling (12), p27 turnover (33), cytokine signaling (14), and growth cone-target interactions (11), it will be interesting to see if isopeptidase activity of Csn5 underlies these diverse processes as well.

All neddylated proteins known are members of the cullin family. It is not clear whether CSN isopeptidase acts exclusively upon cullin-Nedd8 conjugates or cleaves other targets. Regardless, given the large number of F-box proteins and the potential for substantial diversity in the substrates for SCF and other cullin-based ubiquitin ligases, CSN deneddylase activity may play an enormous role in cellular regulation.

References and Notes

1. D. Skowrya, K. L. Craig, M. Tyers, S. J. Elledge, J. W. Harper, *Cell* **91**, 209 (1997).
2. R. M. Feldman, C. C. Correll, K. B. Kaplan, R. J. Deshaies, *Cell* **91**, 221 (1997).
3. R. J. Deshaies, *Annu. Rev. Cell Dev. Biol.* **15**, 435 (1999).
4. F. Osaka *et al.*, *EMBO J.* **19**, 3475 (2000).
5. T. Kawakami *et al.*, *EMBO J.* **20**, 4003 (2001).
6. S. Lyapina *et al.*, *Science* **292**, 1382 (2001).
7. C. Schwechheimer *et al.*, *Science* **292**, 1379 (2001).
8. M. Seeger, C. Gordon, W. Dubiel, *Curr. Biol.* **11**, R643 (2001).
9. N. Wei, X. W. Deng, *Trends Genet.* **15**, 98 (1999).
10. S. Freilich *et al.*, *Curr. Biol.* **9**, 1187 (1999).
11. G. S. Suh *et al.*, *Neuron* **33**, 35 (2002).
12. F. X. Claret, M. Hibi, S. Dhut, T. Toda, M. Karin, *Nature* **383**, 453 (1996).
13. R. Kleemann *et al.*, *Nature* **408**, 211 (2000).
14. E. Bianchi *et al.*, *Nature* **404**, 617 (2000).
15. G. Cope, R. Deshaies, unpublished data.
16. C. Zhou *et al.*, *BMC Biochem.* [online] **2**, article #7 (2001). Available at: www.biomedcentral.com/bmcbiochem.
17. S. F. Altschul *et al.*, *Nucleic Acids Res.* **25**, 3389 (1997).
18. L. Aravind, C. P. Ponting, *Protein Sci.* **7**, 1250 (1998).
19. K. E. Mundt *et al.*, *Curr. Biol.* **9**, 1427 (1999).
20. C. P. Ponting, L. Aravind, J. Schultz, P. Bork, E. V. Koonin, *J. Mol. Biol.* **289**, 729 (1999).
21. N. D. Rawlings, A. J. Barrett, *Methods Enzymol.* **248**, 183 (1995).
22. Like JAMM, metal-dependent peptidases often possess two conserved acidic residues: one that acts as a ligand for zinc and a second that acts as a nucleophile to promote attack by water on the peptide backbone. Based on the common occurrence of Glu as a nucleophile and on the predicted secondary structure of the Jab/MPN domain, we propose that the Glu helps polarize a water molecule for hydrolytic attack and the COOH-terminal His and Asp residues serve as three ligands for zinc.
23. N. Wei, X. W. Deng, *Photochem. Photobiol.* **68**, 237 (1998).

24. A. G. Loewy *et al.*, *J. Biol. Chem.* **268**, 9071 (1993).
25. D. R. Holland, A. C. Hausrath, D. Juers, B. W. Matthews, *Protein Sci.* **4**, 1955 (1995).
26. M. Gomez-Ortiz, F. X. Gomis-Ruth, R. Huber, F. X. Aviles, *FEBS Lett.* **400**, 336 (1997).
27. D. Lammer *et al.*, *Genes Dev.* **12**, 914 (1998).
28. D. Liakopoulos, G. Doenges, K. Matuschewski, S. Jentsch, *EMBO J.* **17**, 2208 (1998).
29. A. C. Gavin *et al.*, *Nature* **415**, 141 (2002).
30. V. N. Podust *et al.*, *Proc. Natl. Acad. Sci. U.S.A.* **97**, 4579 (2000).
31. Null mutant survival up to third instar larvae was context dependent. Although Csn5-null larvae rarely survived to third instar at UCLA, we routinely found that these mutants survived to third instar at CalTech.
32. R. Verma *et al.*, *Science* **298**, 611 (2002).
33. K. Tomoda, Y. Kubota, J. Kato, *Nature* **398**, 160 (1999).
34. Single-letter abbreviations for the amino acid residues are as follows: A, Ala; C, Cys; D, Asp; E, Glu; F, Phe; G, Gly; H, His; I, Ile; K, Lys; L, Leu; M, Met; N, Asn; P, Pro; Q, Gln; R, Arg; S, Ser; T, Thr; V, Val; W, Trp; and Y, Tyr.

35. C. Notredame, D. G. Higgins, J. Heringa, *J. Mol. Biol.* **302**, 205 (2000).
36. B. Rost, C. Sander, R. Schneider, *Comput. Appl. Biosci.* **10**, 53 (1994).
37. Materials and Methods are available as supporting material on *Science Online*.
38. We thank D. Wolf, M. Hochstrasser, K. Mundt, and A. Carr for generously providing yeast strains and plasmids, the S. Benzer lab for providing lab equipment and space, and S. Lyapina for psCSN. We thank members of the Deshaies lab for providing helpful insight and discussions. This work was supported by NIH (G.A.C.) and the Howard Hughes Medical Institute.

Supporting Online Material

www.sciencemag.org/cgi/content/full/1075901/DC1
Materials and Methods
Figs. S1 and S2
References and Notes

9 July 2002; accepted 7 August 2002
Published online 15 August 2002;
10.1126/science.1075901
Include this information when citing this paper.

Role of Rpn11 Metalloprotease in Deubiquitination and Degradation by the 26S Proteasome

Rati Verma,¹ L. Aravind,² Robert Oania,¹ W. Hayes McDonald,³ John R. Yates III,³ Eugene V. Koonin,² Raymond J. Deshaies^{1*}

The 26S proteasome mediates degradation of ubiquitin-conjugated proteins. Although ubiquitin is recycled from proteasome substrates, the molecular basis of deubiquitination at the proteasome and its relation to substrate degradation remain unknown. The Rpn11 subunit of the proteasome lid subcomplex contains a highly conserved Jab1/MPN domain-associated metalloisopeptidase (JAMM) motif—EX_nHXHX₁₀D. Mutation of the predicted active-site histidines to alanine (*rpn11AXA*) was lethal and stabilized ubiquitin pathway substrates in yeast. Rpn11^{AXA} mutant proteasomes assembled normally but failed to either deubiquitinate or degrade ubiquitinated Sic1 in vitro. Our findings reveal an unexpected coupling between substrate deubiquitination and degradation and suggest a unifying rationale for the presence of the lid in eukaryotic proteasomes.

Proteolysis by the 26S proteasome proceeds by binding of the ubiquitinated substrate protein to the 19S regulatory particle, followed by its unfolding and translocation into the lumen of the 20S core, where it is degraded by the action of the 20S peptidases (1–3). At some point in this process, the ubiquitin targeting signal is detached from the substrate. It is appealing to envision that this deubiquitination is obligatorily coupled to degradation. Such coupling would render the targeting event irreversible, prevent unproductive turn-

over of ubiquitin, and presumably alleviate steric blockade of the 20S core entry portal by the bulky ubiquitin chain, which is linked by isopeptide bonds. When and where substrate deubiquitination takes place, the identity of the deubiquitinating enzyme (DUB), and whether deubiquitination of a substrate is essential for its degradation by the proteasome are unclear (4, 5).

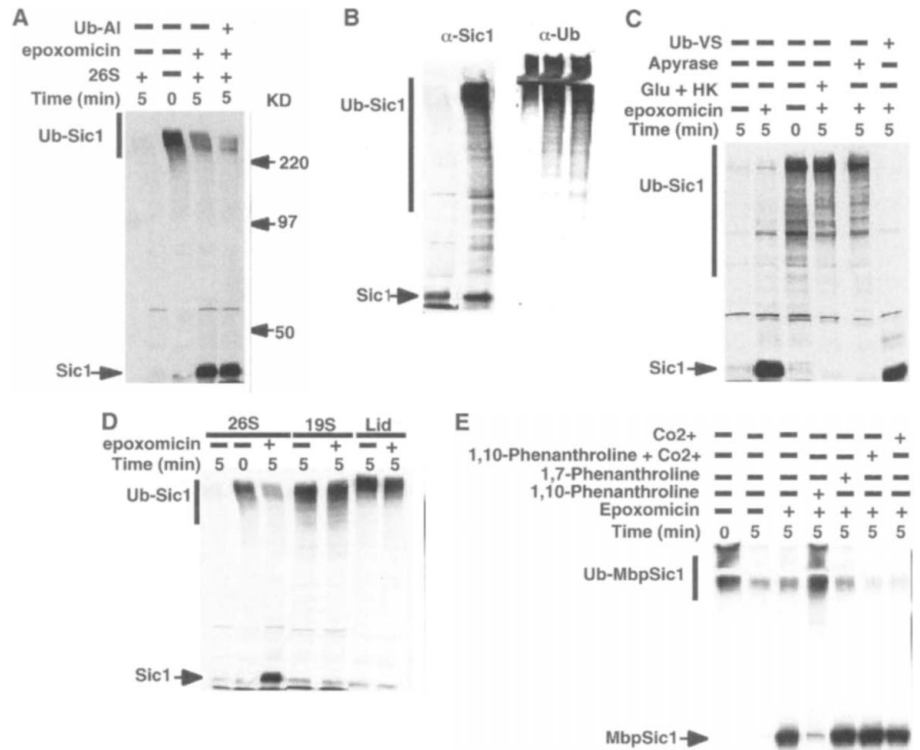
Budding yeast ubiquitinated S-Cdk inhibitor Sic1 (Ub-Sic1) is rapidly degraded by purified 26S proteasomes (3, 6) in a reaction that recapitulates physiological requirements for Sic1 proteolysis (7, 8). To investigate whether degradation of Sic1 is normally accompanied by its deubiquitination, we evaluated the fate of Ub-Sic1 after inhibition of 26S proteolytic activity. Epoxomicin inhibits the proteasome by covalently binding the catalytically active β subunits of the 20S core (9). Purified 26S proteasomes were preincu-

¹Department of Biology and Howard Hughes Medical Institute, California Institute of Technology, Pasadena, CA 91125, USA. ²National Center for Biotechnology Information, National Library of Medicine, National Institutes of Health, Bethesda, MD 20894, USA. ³Department of Cell Biology, The Scripps Research Institute, San Diego, CA 92037, USA.

*To whom correspondence should be addressed. E-mail: deshaies@caltech.edu

REPORTS

Fig. 1. Characterization of Ub-Sic1 deubiquitination by purified 26S proteasomes. (A) Ub-Sic1 is deubiquitinated by epoxomicin-treated 26S proteasomes in a ubiquitin aldehyde-insensitive manner. Purified proteasomes (100 nM) were incubated with either 1% dimethyl sulfoxide (DMSO) (lanes 1 and 2, mock), or 100 μ M epoxomicin in the absence (lane 3) or presence (lane 4) of 2.5 μ M ubiquitin aldehyde (Ub-Al) for 30 min at 30°C. The degradation reaction was initiated by the addition of Ub-Sic1 (300 nM) and 1 \times ATP regenerating system (1 \times ARS) (3), incubated at 30°C for 5 min, and terminated by the addition of SDS sample buffer. Aliquots were resolved by SDS-PAGE (8% polyacrylamide gel), transferred to nitrocellulose, and immunoblotted with polyclonal antibody to Sic1 to monitor degradation. (B) Sic1 generated by epoxomicin-treated proteasomes is completely deubiquitinated. An aliquot of the epoxomicin-treated sample from lane 3 in (A) as well as a Ub-Sic1 preparation containing both Ub-Sic1 and unmodified Sic1 were resolved by SDS-PAGE and immunoblotted with antiserum to Sic1 (α -Sic1) (left) or to ubiquitin (α -Ub) (right). The anti-ubiquitin immunoreactivity is primarily derived from autoubiquitinated Cdc34 (30), which is not degraded (31). (C) Deubiquitination of Ub-Sic1 is ATP dependent. Mock- or epoxomicin-treated 26S proteasomes were depleted of ATP by 5 min of incubation with apyrase (15 units/ml) or hexokinase (5 units/ml) plus 30 mM glucose (Glu + HK) before incubation with Ub-Sic1. Lane 6 is the same as lane 2, except the DUB inhibitor ubiquitin vinyl sulfone (Ub-VS) (32) was included at 2.5 μ M. (D) Subparticles of the 26S proteasome do not efficiently deubiquitinate Ub-Sic1. The 19S regulatory particle was isolated as described in (6). The lid subparticle of 19S was purified from a strain containing *RPN8TEV2MYC9* as described (23). ACoomassie blue-stained preparation is shown in Fig. 4C. The three preparations—26S, 19S, and lid—were incubated in the absence (lanes 1, 2, 4, and 6) or presence (lanes 3, 5, and 7) of epoxomicin and assayed for degradation/



deubiquitination of Ub-Sic1 as described in (A). (E) Inhibition of deubiquitination by the metal chelator 1,10-phenanthroline. 26S proteasomes were preincubated at 30°C with 1% DMSO and 1% MeOH (lanes 1 and 2) or 100 μ M epoxomicin and 1% MeOH (lane 3) containing in addition 1 mM 1,10-phenanthroline (lane 4), 1 mM 1,7-phenanthroline (lane 5), or 1 mM 1,10-phenanthroline premixed with 2 mM CoCl_2 (lane 6) or 2 mM CoCl_2 (lane 7). The degradation reaction was initiated by the addition of Ub-MbpSic1.

A

```

COP9_su5_Hs  NLE.....VGRLENAIGWYHSHPGYGCWLSGIDVSTQMLNQQFQEPFVA--VVIDPRTISAGKVN
Rpn11_Sc     PME.....TGRDQMVVGVYHSHPGFGCWLSSVDVNTQKSFQQLNSRAVA--VVVDPIQSVKQ-KVV
Pad1_Sp     PME.....TGRPEMVVGVYHSHPGFGCWLSSVDINTQQSFEQLTPRAVA--VVVDPIQSVKQ-KVV
Rpn11_C.ele PME.....TGRPEMVVGVYHSHPGFGCWLSSVDINTQQSFEALSDRAVA--VVVDPIQSVKQ-KVV
Poh1_Hs     PME.....TGRPEMVVGVYHSHPGFGCWLSSVDINTQQSFEALSERAVA--VVVDPIQSVKQ-KVV
....E(X)n.....HXHXXXXXXXXXXD
    
```

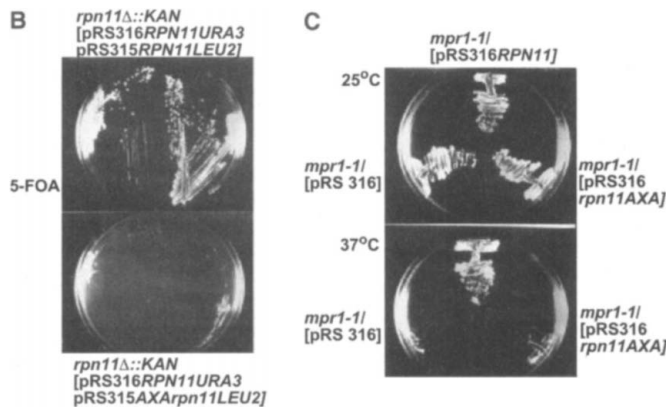


Fig. 2. Rpn11, an intrinsic subunit of the 19S subcomplex of the 26S proteasome, contains a conserved, predicted metalloprotease motif (JAMM) that is critical for viability. (A) Sequence alignment of *RPN11* orthologs with human CSN5/JAB1 reveals the JAMM motif. The multiple alignment was constructed by using the T-Coffee program (33). Each protein is denoted by its name followed by an abbreviated species name. The predicted metal-chelating and catalytic residues are shown as a consensus below the alignment. For a detailed description of the extended JAMM domain consensus based on all *RPN11* orthologs, see fig. S3. (B) An intact JAMM motif is critical for yeast cell proliferation. An *rpn11Δ::KAN* strain kept alive by an [*RPN11 URA3*] plasmid (RJD 1922) was transformed with *LEU2*-marked *RPN11* (RJD 1934) or *rpn11AXA* plasmids (RJD 1935) (23). Transformants (two representative clones each) were streaked onto 5-fluoroorotic acid (FOA) plates and allowed to grow for 5 days at 25°C. Because 5-FOA is toxic to *URA3* cells, growth is observed only when the *URA3*-marked plasmid is rendered dispensable by the *LEU2* plasmid. (C) The *rpn11AXA* mutant cannot complement the *mpr1-1* temperature-sensitive allele of *RPN11*. *mpr1-1* (RJD 1786) was transformed with either empty *PR3316 [URA3]* vector or vector containing wild-type *RPN11* (RJD 1815) or *rpn11AXA* (RJD 1816). Individual transformants were streaked on synthetic minimal (SD)-*Ura* plates and incubated at 25°C or 37°C for 5 days.

bated with or without epoxomicin, Ub-Sic1 was then added, and degradation was monitored by the loss of Sic1 antigen. In the absence of epoxomicin, Ub-Sic1 was completely degraded (Fig. 1A; fig. S1). Surprisingly, in the presence of epoxomicin, a

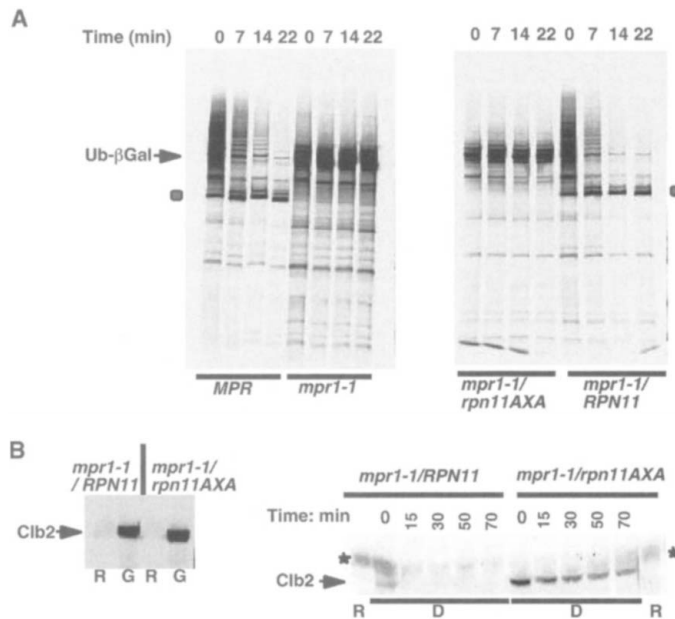
large fraction of Ub-Sic1 molecules were completely deubiquitinated, as judged by comigration with unmodified Sic1 and failure to cross-react with antibodies to ubiquitin (Fig. 1B).

Conversion of Ub-Sic1 to Sic1 differed

from conventional thiol protease-mediated deubiquitination in four respects: (i) it was insensitive to the classic DUB inhibitors ubiquitin aldehyde (Ub-Al) and ubiquitin vinyl sulfone (Ub-VS) (Fig. 1, A and C); (ii) it required adenosine triphosphate (ATP) (Fig.

REPORTS

Fig. 3. An intact JAMM motif is required for degradation of ubiquitin–proteasome pathway substrates in vivo. (A) Stabilization of a UFD pathway substrate in mutant cells. *RPN11* (RJD1901), *mpr1-1* (RJD1902), *mpr1-1 RPN11* (RJD1903), and *mpr1-1 rpn11AXA* (RJD1904) strains (23) containing a reporter plasmid expressing the unstable Ub-V76-Val-eK-B-Gal fusion protein were analyzed by pulse-chase ³⁵S radiolabeling as described in (6). Arrow indicates the ³⁵S-labeled substrate protein, and filled circle shows the position of the 90-kD stable breakdown product of the reporter protein. (B) Stabilization of mitotic cyclin Clb2 in *mpr1-1 rpn11AXA* cells. Mutant *mpr1-1 RPN11* (RJD2002) and *mpr1-1/rpn11AXA* (RJD2004) strains harboring a chromosomally encoded, influenza hemagglutinin antigen (HA)-tagged *GAL-CLB2* expression cassette (23) were grown in raffinose medium (R) at 25°C, and Clb2 expression was induced by the addition of 2% galactose (G). To confirm specific expression of Clb2-HA3, we prepared cell lysates by lysing with glass beads and boiling. Aliquots were resolved by SDS-PAGE, transferred to nitrocellulose, and analyzed by immunoblotting with 12CA5 antibody to HA ascites (left). For evaluation of Clb2-HA3 stability (right), cultures were grown in raffinose (R) medium at 25°C and arrested in G₁ by the addition of α-factor (5 μg/ml) for 2 hours. Clb2 expression was induced with galactose for 1.5 hours, and cultures were shifted to 36°C to inactivate *mpr1-1*. After 1.5 hours, cells were transferred to α-factor-containing dextrose (D) medium at 37°C to extinguish expression of Clb2. Because there is continuous proteolysis of Clb2 in α-factor-arrested cells, and time 0 was collected after washing and resuspension in yeast extract, peptone, and dextrose, the level is much less than that seen in exponential by growing cells (left). Asterisk denotes a nonspecific immunoreactive band to HA.



1C); (iii) it required intact 26S proteasome and was not sustained by 19S regulatory particle or the lid (Fig. 1D); and (iv) it was completely blocked by *o*-phenanthroline (1,10-phenanthroline), but not *m*-phenanthroline (1,7-phenanthroline) or *o*-phenanthroline presaturated with cobalt ions (Fig. 1E). These four properties suggest that a metallopeptidase was responsible for this activity. These properties are reminiscent of an unidentified deubiquitinating activity that copurifies with 26S proteasomes from rabbit reticulocyte lysates (10).

We had characterized our proteasome preparation by mass spectrometry, which revealed only a single known DUB, Ubp6 (3) (table S1). However, Ubp6 was neither necessary nor sufficient for processing Ub-Sic1 (fig. S2). Thus, we reasoned that the DUB activity we observed might reside in a proteasome subunit that harbors a novel ubiquitin isopeptidase activity.

The lid subcomplex of the 19S regulatory particle is necessary for ubiquitin-dependent degradation (11). The lid subunits share sequence conservation with subunits of the COP9 signalosome (CSN). CSN preparations contain an isopeptidase activity that promotes cleavage of the ubiquitin-like molecule

Nedd8 from Nedd8–Cul1 conjugates (12). The Csn5/Jab1 subunit of CSN (13, 14) and the Rpn11 subunit of the lid (Fig. 2A) contain a distinct arrangement of two histidines and an aspartate preceded by a conserved but variably spaced glutamate (EX_nHXHX₁₀D) (15). We refer to this motif as JAMM for Jab1/Pad1/MPN domain metalloenzyme. We propose that the histidines and aspartate bind a zinc ion, which, together with the upstream glutamate, comprise an active site (14).

To evaluate the role of the JAMM motif of Rpn11 in the metal ion-dependent deubiquitination shown in Fig. 1E, we mutated the two conserved histidines to alanines (henceforth referred to as the *rpn11AXA* mutant; table S3). Because Rpn11 is an essential protein (16), we evaluated the effect of the mutation by plasmid shuffling. A haploid *rpn11Δ leu2 ura3* strain sustained by a [*RPN11 URA3*] plasmid was transformed with *LEU2* plasmids containing either *RPN11* or *rpn11AXA*. Transformants that harbored [*rpn11AXA LEU2*] were unable to survive without the [*RPN11 URA3*] plasmid (Fig. 2B), indicating that an intact Rpn11 JAMM motif was critical. To facilitate further phenotypic characterization of the *AXA* mutant, we used *mpr1-1*, which contains a frameshift in *RPN11* that leads to temperature-sensitive

growth and expression of a prematurely terminated Rpn11^{*mpr1-1*} protein (285 versus 306 amino acids for wild type) (16). Plasmid-borne *RPN11* but not *rpn11AXA* complemented the temperature-sensitive growth of *mpr1-1* (Fig. 2C).

Rpn11 and other subunits of the 19S regulatory particle may mediate transcriptional regulation and DNA repair independent of their roles in proteolysis (17, 18). To test whether the inability of *rpn11AXA* to sustain viability might be due to defective protein degradation, we evaluated the stability of an artificial ubiquitin fusion degradation (UFD) pathway substrate (19) and the anaphase-promoting complex/cyclosome substrate Clb2 (20) in wild-type, *mpr1-1*, *mpr1-1/RPN11*, and *mpr1-1/rpn11AXA* cells. For the latter experiment, cells were arrested in the G₁ phase of the cell cycle with α factor, at which time Clb2 proteolysis proceeds rapidly. *RPN11*, but not *rpn11AXA*, complemented the degradation defects observed for both proteins in *mpr1-1* cells (Fig. 3). Thus, the JAMM motif was essential for substrate proteolysis by the 26S proteasome in vivo. Paradoxically, substrates that accumulated in *rpn11AXA* cells were not ubiquitinated. However, when proteolysis is blocked by mutations in proteasome subunits (21) or the DUB Doa4 (22), substrates accumulate primarily in an unmodified form, presumably because of robust activity of “scavenging” DUBs.

To determine the biochemical basis of the *rpn11AXA* degradation defect, we sought to evaluate the activity of Rpn11^{*AXA*} proteasomes in vitro. We affinity-purified proteasomes from an *mpr1-1* strain harboring a chromosomal copy of either *RPN11* or *rpn11AXA* (23). Immunoblotting with anti-serum to Pad1/Rpn11 (24) revealed that extracts from *RPN11* and *mpr1-1* contained full-length and truncated Rpn11, respectively, whereas extracts from the *mpr1-1/RPN11* and *mpr1-1/rpn11AXA* strains contained both polypeptides (Fig. 4A). Fortunately, no truncated Rpn11^{*mpr1-1*} was present in 26S proteasomes prepared from *mpr1-1* strains. This allowed us to prepare point-mutant 26S proteasomes that contained Rpn11^{*AXA*}, with no contamination by Rpn11^{*mpr1-1*}.

Native gel electrophoresis followed by Coomassie blue staining and in-gel peptidase assay with a fluorogenic substrate (Fig. 4E) suggested that proteasomes from *mpr1-1* cells were defective for assembly. Indeed, 26S proteasomes from the *mpr1-1* strain lacked subunits of the lid subcomplex of the 19S regulatory particle as judged by SDS-polyacrylamide gel electrophoresis (PAGE) (Fig. 4, B and C) and mass spectrometry (tables S1 and S2). Thus, the COOH terminus of Rpn11 was required either for stabilization of the lid or for association of the base and lid subcom-

plex (11). The lid subcomplex of the 19S regulatory particle is necessary for ubiquitin-dependent degradation (11). The lid subunits share sequence conservation with subunits of the COP9 signalosome (CSN). CSN preparations contain an isopeptidase activity that promotes cleavage of the ubiquitin-like molecule

Nedd8 from Nedd8–Cul1 conjugates (12). The Csn5/Jab1 subunit of CSN (13, 14) and the Rpn11 subunit of the lid (Fig. 2A) contain a distinct arrangement of two histidines and an aspartate preceded by a conserved but variably spaced glutamate (EX_nHXHX₁₀D) (15). We refer to this motif as JAMM for Jab1/Pad1/MPN domain metalloenzyme. We propose that the histidines and aspartate bind a zinc ion, which, together with the upstream glutamate, comprise an active site (14).

To evaluate the role of the JAMM motif of Rpn11 in the metal ion-dependent deubiquitination shown in Fig. 1E, we mutated the two conserved histidines to alanines (henceforth referred to as the *rpn11AXA* mutant; table S3). Because Rpn11 is an essential protein (16), we evaluated the effect of the mutation by plasmid shuffling. A haploid *rpn11Δ leu2 ura3* strain sustained by a [*RPN11 URA3*] plasmid was transformed with *LEU2* plasmids containing either *RPN11* or *rpn11AXA*. Transformants that harbored [*rpn11AXA LEU2*] were unable to survive without the [*RPN11 URA3*] plasmid (Fig. 2B), indicating that an intact Rpn11 JAMM motif was critical. To facilitate further phenotypic characterization of the *AXA* mutant, we used *mpr1-1*, which contains a frameshift in *RPN11* that leads to temperature-sensitive

growth and expression of a prematurely terminated Rpn11^{*mpr1-1*} protein (285 versus 306 amino acids for wild type) (16). Plasmid-borne *RPN11* but not *rpn11AXA* complemented the temperature-sensitive growth of *mpr1-1* (Fig. 2C).

Rpn11 and other subunits of the 19S regulatory particle may mediate transcriptional regulation and DNA repair independent of their roles in proteolysis (17, 18). To test whether the inability of *rpn11AXA* to sustain viability might be due to defective protein degradation, we evaluated the stability of an artificial ubiquitin fusion degradation (UFD) pathway substrate (19) and the anaphase-promoting complex/cyclosome substrate Clb2 (20) in wild-type, *mpr1-1*, *mpr1-1/RPN11*, and *mpr1-1/rpn11AXA* cells. For the latter experiment, cells were arrested in the G₁ phase of the cell cycle with α factor, at which time Clb2 proteolysis proceeds rapidly. *RPN11*, but not *rpn11AXA*, complemented the degradation defects observed for both proteins in *mpr1-1* cells (Fig. 3). Thus, the JAMM motif was essential for substrate proteolysis by the 26S proteasome in vivo. Paradoxically, substrates that accumulated in *rpn11AXA* cells were not ubiquitinated. However, when proteolysis is blocked by mutations in proteasome subunits (21) or the DUB Doa4 (22), substrates accumulate primarily in an unmodified form, presumably because of robust activity of “scavenging” DUBs.

To determine the biochemical basis of the *rpn11AXA* degradation defect, we sought to evaluate the activity of Rpn11^{*AXA*} proteasomes in vitro. We affinity-purified proteasomes from an *mpr1-1* strain harboring a chromosomal copy of either *RPN11* or *rpn11AXA* (23). Immunoblotting with anti-serum to Pad1/Rpn11 (24) revealed that extracts from *RPN11* and *mpr1-1* contained full-length and truncated Rpn11, respectively, whereas extracts from the *mpr1-1/RPN11* and *mpr1-1/rpn11AXA* strains contained both polypeptides (Fig. 4A). Fortunately, no truncated Rpn11^{*mpr1-1*} was present in 26S proteasomes prepared from *mpr1-1* strains. This allowed us to prepare point-mutant 26S proteasomes that contained Rpn11^{*AXA*}, with no contamination by Rpn11^{*mpr1-1*}.

Native gel electrophoresis followed by Coomassie blue staining and in-gel peptidase assay with a fluorogenic substrate (Fig. 4E) suggested that proteasomes from *mpr1-1* cells were defective for assembly. Indeed, 26S proteasomes from the *mpr1-1* strain lacked subunits of the lid subcomplex of the 19S regulatory particle as judged by SDS-polyacrylamide gel electrophoresis (PAGE) (Fig. 4, B and C) and mass spectrometry (tables S1 and S2). Thus, the COOH terminus of Rpn11 was required either for stabilization of the lid or for association of the base and lid subcom-

REPORTS

plexes in vitro. By contrast, proteasomes recovered from both *mpr1-1/RPN11* and *mpr1-1/rpn11AXA* cells were assembled into functional particles as judged by native gel electrophoresis (Fig. 4E), denaturing SDS-PAGE (Fig. 4B), and immunoblot analysis (Fig. 4D) and contained all 26S subunits as determined by mass spectrometry (table S1).

The "isogenic" Rpn11- and Rpn11^{AXA}-containing 26S proteasomes were next tested for their ability to deubiquitinate and degrade Ub-Sic1. As expected, Rpn11-containing 26S proteasomes degraded Ub-Sic1, and preincubation with epoxomicin blocked degradation,

leading to the accumulation of deubiquitinated Sic1 (Fig. 4F). In contrast, the Rpn11^{AXA} 26S proteasomes were profoundly defective for both activities. This result suggests a compelling biochemical rationale for the lethality of *rpn11AXA*.

We envision the following sequence of steps in the degradation cycle. After binding of a multiubiquitinated substrate to the 26S proteasome, the substrate is unfolded and threaded into the 20S core. Concomitantly, the substrate is deubiquitinated by the metalloisopeptidase activity of Rpn11. If Rpn11 activity is blocked, we envision that the tetraubiquitin chain targeting signal, which has a diameter of about 28 Å

(as deduced from the crystal structure coordinates in the Protein Data Bank), would sterically block further substrate translocation upon collision with the entry portal of the 20S proteasome, which has a diameter comparable to that reported for *Thermoplasma acidophilum* (13 Å) (25). Substrate deubiquitination by Rpn11 thus defines a new, key step in protein degradation by 26S proteasome. Because deubiquitination of Ub-Sic1 requires ATP and is not sustained by a free lid or 19S regulatory particle, we propose that deubiquitination of a substrate is normally coupled tightly to its translocation into the 20S core. Although the mechanism underlying this coupling is unknown, we posit that it renders degradation vectorial by preventing deubiquitination until the substrate is irreversibly committed to proteolysis.

Eukaryotic proteasomes are distinguished from bacterial and archaeal ATP-dependent proteases primarily by their dependence on ubiquitin and the presence of the lid subcomplex (26). Highly specific targeting of substrates can be mediated by prokaryotic adenosine triphosphatases (ATPases) (27, 28), and Rpt5 ATPase appears to be the proteasomal receptor for ubiquitin chains (29). Taken together, these observations raise the question of why eukaryotic proteasomes have a lid. A unifying simplification emerges if one considers that a major—and perhaps only—function of the lid is to serve as a specialized isopeptidase that tightly couples the deubiquitination and degradation of substrates.

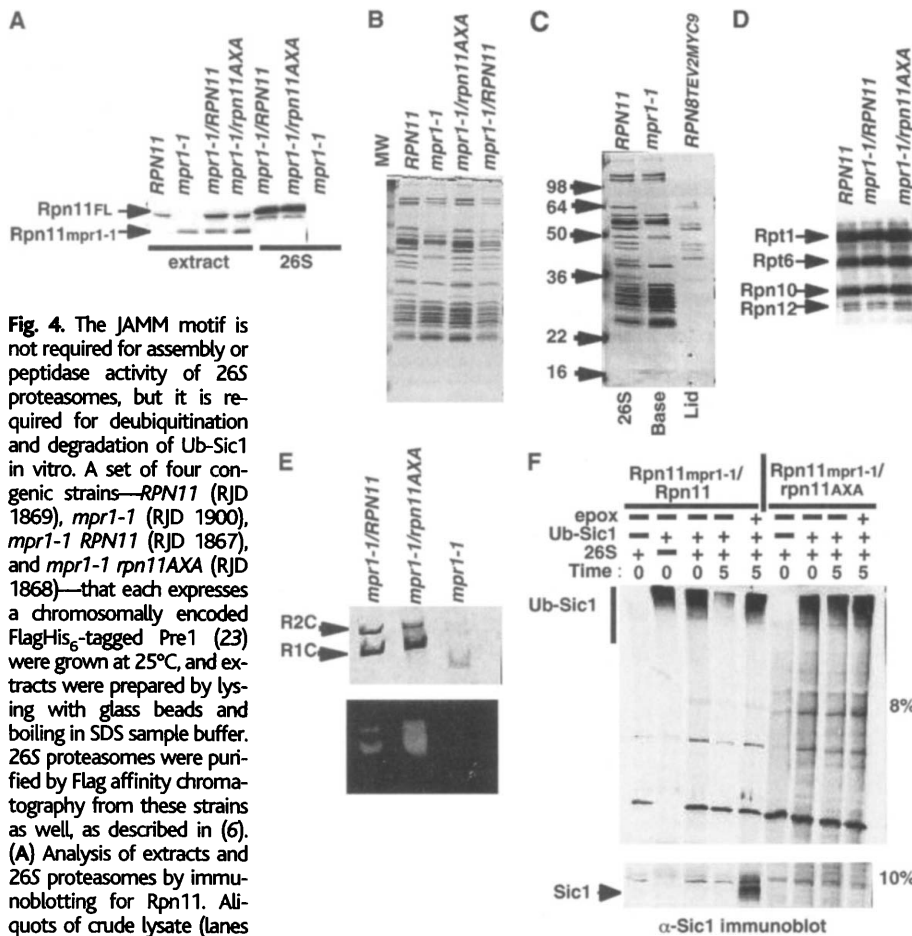


Fig. 4. The JAMM motif is not required for assembly or peptidase activity of 26S proteasomes, but it is required for deubiquitination and degradation of Ub-Sic1 in vitro. A set of four congenic strains—*RPN11* (RJD 1869), *mpr1-1* (RJD 1900), *mpr1-1 RPN11* (RJD 1867), and *mpr1-1 rpn11AXA* (RJD 1868)—that each expresses a chromosomally encoded FlagHis₆-tagged Pre1 (23) were grown at 25°C, and extracts were prepared by lysing with glass beads and boiling in SDS sample buffer. 26S proteasomes were purified by Flag affinity chromatography from these strains as well, as described in (6). (A) Analysis of extracts and 26S proteasomes by immunoblotting for Rpn11. Aliquots of crude lysate (lanes 1 to 4) and purified proteasomes (lanes 5 to 7) were resolved by SDS-PAGE, transferred to nitrocellulose, and immunoblotted with antiserum to Pad1, the *Schizosaccharomyces pombe* Rpn11 ortholog (24). (B and C) *mpr1-1* but not *rpn11AXA* mutation alters polypeptide composition of 26S proteasome. Proteasomes isolated from the indicated strains were fractionated by SDS-PAGE and stained with Coomassie blue. The lid subparticle shown in (C) was purified as described in (23). (D) *rpn11AXA* mutation does not perturb assembly of the 19S regulatory particle. Purified 26S proteasomes were evaluated by immunoblotting with antibodies specific for the indicated proteasome subunits. (E) The *mpr1-1* but not *rpn11AXA* mutation compromises assembly and peptidase activity of 26S proteasome. Purified 26S proteasomes were resolved by electrophoresis on a 4% nondenaturing polyacrylamide gel and analyzed by Coomassie blue staining (top) or in-gel peptidase activity by incubating with the fluorescent peptidase substrate Suc-LLVY-AMC, as described in (6). (F) Point-mutant proteasomes with an altered JAMM motif are unable to deubiquitinate and degrade Ub-Sic1 in vitro. 26S proteasomes were prepared by anti-Flag affinity chromatography from RJD 1867 (*mpr1-1 RPN11*) and RJD 1868 (*mpr1-1 rpn11AXA*) cells expressing a chromosomally encoded FlagHis₆-tagged Pre1. Purified proteasomes were incubated with 2.5 μM ubiquitin aldehyde at 30°C in the presence or absence of 100 μM epoxomicin. Ub-Sic1 and ATP-regenerating system were then added, and degradation was monitored as described in Fig. 1. Lanes 1 and 6 contain the 26S proteasome preparations from *mpr1-1 RPN11* and *mpr1-1 rpn11AXA*, respectively, with no Ub-Sic1 added. The same samples were run on an 8% gel (top) as well as a 10% gel (bottom) to better visualize the Ub-Sic1 conjugates and unmodified Sic1.

References and Notes

1. A. Hershko, A. Ciechanover, *Annu. Rev. Biochem.* **67**, 425 (1998).
2. J. Thrower, L. Hoffman, M. Rechsteiner, C. Pickart, *EMBO J.* **19**, 94 (2000).
3. R. Verma, H. McDonald, J. R. Yates III, R. J. Deshaies, *Mol. Cell* **8**, 439 (2001).
4. K. D. Wilkinson, M. Hochstrasser, in *Ubiquitin and the Biology of the Cell*, J. Peters, J. Harris, D. Finley, Eds. (Plenum Press, New York, 1998), pp. 99–125.
5. C. H. Chung, S. H. Baek, *Biochem. Biophys. Res. Commun.* **266**, 633 (1999).
6. R. Verma *et al.*, *Mol. Biol. Cell* **11**, 3425 (2000).
7. E. Schwob, T. Böhm, M. Mendenhall, K. Nasmyth, *Cell* **79**, 233 (1994).
8. R. Verma *et al.*, *Science* **278**, 455 (1997).
9. L. Meng *et al.*, *Proc. Natl. Acad. Sci. U.S.A.* **96**, 10403 (1999).
10. E. Eytan, T. Armon, H. Heller, S. Beck, A. Hershko, *J. Biol. Chem.* **268**, 4668 (1993).
11. M. Glickman *et al.*, *Cell* **94**, 615 (1998).
12. S. Lyapina *et al.*, *Science* **292**, 1382 (2001).
13. C. P. Ponting, L. Aravind, J. Schultz, P. Bork, E. V. Koonin, *J. Mol. Biol.* **289**, 729 (1999).
14. G. A. Cope *et al.*, *Science* **298**, 608 (2002).
15. Single-letter abbreviations for the amino acid residues are as follows: A, Ala; C, Cys; D, Asp; E, Glu; F, Phe; G, Gly; H, His; I, Ile; K, Lys; L, Leu; M, Met; N, Asn; P, Pro; Q, Gln; R, Arg; S, Ser; T, Thr; V, Val; W, Trp; and Y, Tyr.
16. T. Rinaldi, C. Ricci, D. Porro, M. Bolotin-Fukuhara, L. Frontali, *Mol. Biol. Cell* **9**, 2917 (1998).
17. R. C. Conaway, C. S. Brower, J. W. Conaway, *Science* **296**, 1254 (2002).
18. M. L. Stitzel, R. Durso, J. C. Reese, *Genes Dev.* **15**, 128 (2001).
19. E. S. Johnson, B. Bartel, W. Seufert, A. Varshavsky, *EMBO J.* **11**, 497 (1992).

REPORTS

20. A. Amon, S. Irmiger, K. Nasmyth, *Cell* **77**, 1037 (1994).
 21. W. Seufert, S. Jentsch, *EMBO J.* **11**, 3077 (1992).
 22. F. R. Papa, M. Hochstrasser, *Nature* **366**, 313 (1993).
 23. Materials and methods are available as supporting material on Science Online.
 24. M. Shimanuki, Y. Saka, M. Yanagida, T. Toda, *J. Cell Sci.* **108**, 569 (1995).
 25. M. Groll *et al.*, *Nature Struct. Biol.* **7**, 1062 (2000).
 26. D. Voges, P. Zwickl, W. Baumeister, *Annu. Rev. Biochem.* **68**, 1015 (1999).
 27. C. K. Smith, T. A. Baker, R. T. Sauer, *Proc. Natl. Acad. Sci. U.S.A.* **96**, 6678 (1999).
 28. R. Verma, R. J. Deshaies, *Cell* **101**, 341 (2000).
 29. Y. A. Lam, T. G. Lawson, M. Velayutham, J. L. Zweier, C. M. Pickart, *Nature* **416**, 763 (2002).
 30. J. Seol *et al.*, *Genes Dev.* **13**, 1614 (1999).
 31. R. Verma, unpublished observations.
 32. A. Borodovsky *et al.*, *EMBO J.* **20**, 5187 (2001).
 33. C. Notredame, D. G. Higgins, J. Heringa, *J. Mol. Biol.* **302**, 205 (2000).
 34. This work was supported by Howard Hughes Medical Institute (R.V. and R.J.D.) and by a grant to University of Washington (W.H.M. and J.R.Y., UOW/RR11823-05-01). We are indebted to C. Crews for epoxomicin, K. Takeda and T. Toda for antiserum to pad1/Rpn11, T. Rinaldi for the MPR and mpr1-1 strains, M. Hochstrasser for ubp6Δ, C. H. Chung for Ubp6 antiserum,

G. Alexandru and K. Nasmyth for the GAL-CLB2-HA3 strain, and the Deshaies lab members for critical comments.

Supporting Online Material

www.sciencemag.org/cgi/content/full/1075898/DC1

Materials and Methods

Figs. S1 to S3

Tables S1 to S3

9 July 2002; accepted 7 August 2002

Published online 15 August 2002;

10.1126/science.1075898

Include this information when citing this paper.

Impacts of Soil Faunal Community Composition on Model Grassland Ecosystems

M. A. Bradford,^{1*} T. H. Jones,² R. D. Bardgett,³ H. I. J. Black,⁴ B. Boag,⁵ M. Bonkowski,⁶ R. Cook,⁷ T. Eggers,¹ A. C. Gange,⁸ S. J. Grayston,⁹ E. Kandeler,¹⁰ A. E. McCaig,^{11†} J. E. Newington,¹ J. I. Prosser,¹¹ H. Setälä,¹² P. L. Staddon,^{13‡} G. M. Tordoff,¹ D. Tschërko,¹⁰ J. H. Lawton^{1,14}

Human impacts, including global change, may alter the composition of soil faunal communities, but consequences for ecosystem functioning are poorly understood. We constructed model grassland systems in the Ecotron controlled environment facility and manipulated soil community composition through assemblages of different animal body sizes. Plant community composition, microbial and root biomass, decomposition rate, and mycorrhizal colonization were all markedly affected. However, two key ecosystem processes, aboveground net primary productivity and net ecosystem productivity, were surprisingly resistant to these changes. We hypothesize that positive and negative faunal-mediated effects in soil communities cancel each other out, causing no net ecosystem effects.

Soil fauna are essential to efficient nutrient cycling, organic matter turnover, and maintenance of soil physical structure, processes that are key determinants of primary production and ecosystem carbon storage (1–3). Consequently, there is considerable concern about impacts on ecosystem functioning that might result from shifts in the community composition of soil fauna mediated through global change (4–6). Predictions based on theoretical considerations of soil communities are ambivalent. Indeterminate and unexpected impacts are predicted from food web theory (7, 8). Redundancy is also postulated to be common (9), with large changes in community composition having minimal effects. Anderson (10) argued that net effects may be positive, negative, or zero, depending on the balance between sink and source processes operating at finer scales. Keystone species theory (11) and distinct bacterial versus fungal energy channels (12, 13) further cloud the predictions. Therefore, an empirical approach is essential for predicting the impacts of shifts in soil community composition on ecosystem functioning.

Pot experiments with soil, soil organisms, and sometimes an individual plant or plant species have demonstrated the marked potential effects of loss of specific soil fauna and faunal groups on a range of ecosystem processes (14–16). However, the validity of extrapolating these studies to the field is questionable given the low species numbers of soil fauna and plants (if present) typically used, the artificiality of the soil, and the limited number of variables measured. What is required is an approach that manipulates the composition of a soil faunal community with a species richness more akin to that in the field, which includes a multispecies plant community and a reconstructed soil profile and measures the response of a suite of interacting variables. To manipulate the soil community in the field, and maintain it over biologically meaningful temporal and spatial scales, is logistically difficult (17). Ecological microcosms make such investigations eminently more feasible. We used the Ecotron controlled environment facility (18) to test the role of one component of soil community composition—namely, assemblages that dif-

fer in animal body sizes—on carbon flux, and microbial and plant community composition and abundance.

We constructed 15 terrestrial microcosms over a period of 7 months (19) as analogs of a temperate, acid, sheep-grazed grassland (a habitat that occurs widely across the upland regions of northern Britain). We maintained the microcosms in the Ecotron under constant environmental conditions (19) for a further 8.5 months. Soil, plants, fauna, and microorganisms for microcosm construction were collected from the grassland (19). Soil fauna were assigned to a functional group according to body width (20, 21) of the adult or, if the adult was not soil dwelling, largest larval stage. Body size provides a good functional classification because it correlates with metabolic rate, generation time, population density, and food size (22).

¹Natural Environment Research Council Centre for Population Biology, Department of Biological Sciences, Imperial College at Silwood Park, Ascot, SL5 7PY, UK. ²Biodiversity and Ecological Processes Research Group, Cardiff School of Biosciences, Cardiff University, Post Office Box 915, Cardiff, CF10 3TL, UK. ³Department of Biological Sciences, Institute of Environmental and Natural Sciences, Lancaster University, Lancaster, LA1 4YQ, UK. ⁴Centre for Ecology and Hydrology, Merlewood, Grange-over-Sands, LA11 6JU, UK. ⁵Scottish Crop Research Institute, Invergowrie, Dundee, DD2 5DA, UK. ⁶Technische Universität Darmstadt, Fachbereich 10, Biologie, D-64287 Darmstadt, Germany. ⁷Institute of Grassland and Environmental Research, Plas Gogerddan, Aberystwyth, SY23 3EB, UK. ⁸School of Biological Sciences, Royal Holloway, University of London, Egham, TW20 0EX, UK. ⁹Macaulay Land Use Research Institute, Craigiebuckler, Aberdeen, AB15 8QH, UK. ¹⁰Institute of Soil Science, University of Hohenheim, 70599 Stuttgart, Germany. ¹¹Department of Molecular and Cell Biology, University of Aberdeen, Institute of Medical Sciences, Foresterhill, Aberdeen, AB25 2ZD, UK. ¹²Department of Ecological and Environmental Sciences, University of Helsinki, Niemenkatu 73, FIN-15140 Lahti, Finland. ¹³Department of Biology, University of York, Post Office Box 373, York, YO10 5YW, UK. ¹⁴Natural Environment Research Council, Polaris House, North Star Avenue, Swindon, SN2 1EU, UK.

*To whom correspondence should be addressed. E-mail: m.a.bradford@ic.ac.uk

†Present address: Engineering and Physical Sciences Research Council, Polaris House, North Star Avenue, Swindon, SN2 1ET, UK.

‡Present address: Plant Research Department, Risø National Laboratory, Postbox 49, Roskilde, DK-4000, Denmark.